Superinfection, Metapopulation Dynamics, and the Evolution of Diversity

Robert M. May and Martin A. Nowak

Department of Zoology, University of Oxford, South Parks Road, OX1 3PS, Oxford, U.K.

Using both analytic and numerical methods, we elucidate the dynamical properties of a class of metapopulation models in which many different species/strains contend for persistence, with local extinction of subpopulations being balanced by colonization of other patches. The species/strains have a strict competitive hierarchy with a given species/strain "taking over" any patch occupied by a lower-ranking species/strain; competitively inferior species/strains compensate by having higher colonization rates and/or lower patch death rates. New species/strains keep appearing, so that we can follow the evolution of the system. Such models may be metaphors for multispecies metapopulations, or for the evolution of virulence (where the patches are hosts, who are infected with various strains of a pathogen, and then die or recover at strain-dependent rates).

Our emphasis is on a set of questions relating to the evolution of diversity. How many species/strains are present after a long time, t? Asymptotically, this number continues to increase very slowly, as $\ln t$. What are the relative abundances of the species/strains? Under a broad range of assumptions about the mutations which produce new species/strains, the rank-abundance distribution is roughly geometric (as is commonly observed in early succession and other "ecologically one-dimensional" situations); some of our analysis here is based in part on an interesting but unproved mathematical conjecture about a new kind of probabilistic/combinatorial problem. If the number of patches/hosts is permanently reduced—by habitat destruction or vaccination—what happens? Characteristically, there is an initial sharp loss of species/strains (with selective removal of the competitive dominants), with subsequent slow recovery as new mutants continue to partition the now-diminished "niche space" (but the pristine levels of virulence are not regained).

1. Introduction

Recently we have developed a model (Nowak & May, 1994) which enables us to explore the evolution of virulence in host–parasite associations, in those situations where superinfection can occur. Most of the rising tide of publications on the evolution of virulence is restricted to circumstances in which individual hosts can be infected with only one strain, so that, overall, the strain with the highest intrinsic reproductive rate, R_0, will eventually exclude all others; the emphasis is then on the constraining relations between virulence (which we define as mortality due to infection) and transmissibility, and on the consequent implications for long-term patterns in the evolution of

virulence. But things are clearly more complicated if many different strains—with different virulences and transmissibilities—can "co-infect" a single host. Superinfection represents an intermediate level of complexity: here a more virulent strain of infection can "take over" a host that is already infected with a less virulent strain, but the host will, in effect, harbour only one strain of infection at any one time. Thus superinfection models go beyond single infection ones in allowing for intra-host competition among strains, but they stop short of the full complexity of co-infection by assuming a form of competitive dominance hierarchy among strains within hosts. We plan a more comprehensive study of general models of co-infection (Nowak & May, in preparation).

Bremermann & Pickering (1983) looked at competition among parasite strains within a host, concluding that selection will always favour the most virulent strain. Levin & Pimentel (1981) studied superinfection in a two-strain model, finding conditions under which co-existence was possible. Anderson & May (1986) extended the analysis of this two-strain model, with explicit attention to the results of invasion of a pathogen–host system by a more virulent strain capable of superinfection; these authors also discussed the history of Dutch elm disease (the fungus *Ceratocystis ulmi*) in the UK, and of myxoma virus among Australian rabbits, in the light of their model. Nowak & May (1994) used analytic methods coupled with extensive numerical simulations to examine superinfection in models with an arbitrarily large number of strains, and also with new strains continually appearing by mutation. They concluded, broadly, that the effects of superinfection are: (i) an increase in the average level of virulence (above that which maximises R_0; the strain with the highest R_0 may even become extinct); (ii) polymorphism of parasite strains, with many different levels of virulence, within a well-defined range; (iii) possible maintenance of strains with levels of virulence so high that they could not persist alone in an otherwise uninfected host population (i.e. strains with $R_0 < 1$); and (iv) very complicated dynamics, possibly including heteroclinic cycles and sudden large changes in the average level of virulence. The focus of all this earlier work is on patterns in the evolution of virulence. For a more full discussion and review, see Nowak & May (1994).

Independently, Tilman (1994) has studied the dynamics of multispecies metapopulation models, in which there is a hierarchy of competitive dominance among the species. Such metapopulation models consider species whose overall populations persist by virtue of a shifting balance of local extinctions and recolonizations of subpopulations among a large number of habitat patches. Tilman's work builds on Hastings' (1980) and Nee & May's (1992) examinations of a two-species such metapopulation model, in which the competitively dominant species always "took over" any patch in which both species occurred, but where the inferior competitor had a compensating advantage of a larger colonization rate and/or a lower patch death-rate.

Nee & May (1992) were interested in the effects of destroying some fraction of the original number of patches, and they showed that such "habitat destruction" favoured the inferior competitor, whose overall abundance could even be increased by weak-to-intermediate levels of disturbance. Tilman (1994) has extended this analysis to multispecies situations, exploring how total species numbers and relative abundances are influenced by patch removal. Tilman also has made the important observation that there are, in effect, "limits to similarity" among species who co-exist in such multispecies metapopulations: a species can invade and persist only if its colonization and patch death rates lie in a narrowly defined range, determined by its place in the hierarchy of competitive dominance and by the parameters characterizing the other species in the ensemble. We also refer to Metz & Dieckman (1986) for models on metapopulations.

Our earlier work (Nowak & May, 1994) and Tilman's (1994) multispecies metapopulation models have an identical mathematical structure. This is not surprising. Like Tilman's metapopulation models, the superinfection models are derived from simplifying more general "co-infection" models, by assuming a strict hierarchy of competitive dominance (measured by ability to "take over" a host or patch). In the superinfection models we have many different strains of infection, which occupy or infect different hosts; hosts die (at rates which combine a background rate with infection-specific effects), and newly infected hosts are produced at rates which depend on the transmission efficiency of the infection in an infected host. Each aspect has its analogue in the multispecies metapopulation models, where many species are distributed among habitat patches, which revert to emptiness (at rates which depend on background effects and possibly on species-specific effects), and which send out new colonizers at rates which differ from species to species. Against these structural and formal equivalences, there are differences of detail which derive from differences in biological details and emphases. Our superinfection models tend to emphasize differences in virulence (i.e. disease-induced host death rate); for simplicity, we often assume that all strains are equally transmissible (Nowak & May, 1994). In contrast, Tilman's (1994) metapopulation studies tend to emphasize differences in colonizing ability (with the inferior competitors having higher "transmission rates"); for simplicity, Tilman often assumes a constant patch-death rate, independent of which species occupies the patch.

In the present paper, we extend our earlier analysis of superinfection, and also explicitly relate it to multispecies metapopulation models. The emphasis in Nowak & May (1994) was mainly on the evolution of virulence. In the present paper, our emphasis is more on a set of questions related to the evolution of diversity. Regardless of whether the mathematical models are oriented towards superinfection or towards metapopulations, we ask questions such as: How many strains/species are present? How does this

number change, over time, as new mutations arise? What are the relative abundances of the strains/ species? If the total number of hosts/patches is reduced—by vaccination or by habitat destruction— what are the likely consequences? As before, we elucidate the dynamical behaviour of our mathematical models by a combination of numerical simulations and analytic results for representative special cases.

Specifically, the paper is organized as follows. In Section 2, we set out the basic set of equations for the dynamics of our n-species system. Section 3 gives an explicit and general solution for the equilibrium abundances of the n-strains/species, for the interesting special case where the superinfection coefficient is unity ($s = 1$). In particular, explicit expressions for the equilibrium abundances, y_i, are given for the limiting cases when all strains/species have the same transmission or colonization coefficient (case I, $b_i = b$ = constant), and when all have the same virulence or patch death rate (case II, $v_i = v_0$ = constant). Section 4 widens the discussion, to investigate new strains/species arising by mutation or otherwise, and consequently to study the average abundance of any one strain/species, $y(v)$, as a function of virulence, v (or other relevant parameters); the average number of strains/species, $\rho(v)\,dv$, between v and $v + dv$; and the average total abundance of all strains/species in the neighbourhood of v, $x(v) = y(v)\rho(v)$. In Section 5, we give explicit expressions for the average total abundance, $x(v)$, for the interesting limiting cases I and II (defined above and in Section 3). Section 6 derives a general analytic expression for the asymptotic ($n \gg 1$) density of strains/species, $\rho(v)$, as a function of the probability that a new mutant strain/species will appear at v; this expression is partly based on a plausible, but unproven, conjecture about the dynamics of these systems (specifically, about the probability that invasion by a new strain at v will lead to extinction of an already-existing strain at v'). Specific expressions are then given for interesting special cases (e.g. new mutants appearing uniformly randomly along the v-axis). By integrating $\rho(v)$, we can calculate the total number of strains/species, and from the relation $x(v) = y(v)\rho(v)$ we can calculate the average abundances of individual strains, $y(v)$, once $x(v)$ and $\rho(v)$ are known (Section 7). Section 8 compares these analytic results for $x(v)$, $\rho(v)$ and $y(v)$ with extensive numerical simulations, for both cases I and II, and for various assumptions about the probability distribution of new mutant strains/species.

Focusing more on the biological implications of the results, Section 9 discusses briefly the kinds of patterns of species' relative abundance that are implied by the results of Sections 6, 7 and 8. Section 10 assumes that new strains/species continue to appear, at some uniform rate, and investigates the number of species, $n(t)$, expected to be found in total in these systems, after time t has elapsed (remember, not all mutants will establish themselves, and those that do will cause some "reshuffling" and loss of existing species). Section 11 studies the effects of vaccination (which effectively reduces the total number of hosts) or habitat destruction (which reduces the total number of available patches). Finally, Section 12 summarizes the main conclusions.

Throughout, the emphasis in the present paper is on mathematical results. We plan a shorter and more biologically oriented review and discussion of the main conclusions, directed toward a broader audience (May, R. M., Nowak, M. A. and Tilman, D., in preparation).

2. The Basic Superinfection or Metapopulation Model

As set out by Nowak & May [1994: eqn (9)], and in different notation by Tilman (1994), our basic model is

$$\frac{dy_i}{dt} = y_i\left[b_i y_0 - u - v_i + sb_i \sum_{j=1}^{i-1} y_j - s \sum_{j=i+1}^{n} b_j y_j \right]. \quad (1)$$

Here y_i is the proportion of hosts infected with the strain labelled i, or, equivalently, is the fraction of all patches which contain species $i (i = 1, 2, 3, \ldots, n)$. Uninfected hosts or empty patches constitute a fraction y_0. We assume the total number of hosts or patches, K, is a fixed constant, so that $\sum_{i=0}^{n} y_i = 1$. The parameter b_i represents the transmission efficiency of strain/species i, so that—assuming homogeneous mixing among the ensemble of hosts or patches—the probability (per unit time) that an empty patch will be colonized by species i is proportional to b_i and to the fraction of patches occupied by i (and thus producing colonizing propagules), y_i; hence the net rate at which new infections with strain/species i appear is $b_i y_i y_0$. By the same token, new infections with species i appear by superinfection at a rate $sb_i y_i \sum_{j=1}^{i-1} y_j$, as encounters arise at a rate $b_i y_i$ with hosts infected by strains/species lower in the dominance hierarchy (y_j with $j < i$). The "superinfection coefficient", s, describes the relative probability of superinfection arising, compared with the infection of uninfected hosts (see Nowak & May, 1994, for fuller discussion). For example, if $s = 1$ then superinfection of an already infected host occurs at the same rate (with the same probability) as infecting an uninfected host. If $s < 1$ then superinfection is slower. If $s = 0$ then superinfection is impossible. If $s > 1$ then already infected hosts

will acquire a second infection more easily. The term $-syi\,\Sigma_{j=i+1}^{n}\,b_j y_j$ represents the rate of loss of hosts infected with strain i, as a result of superinfection by "competitively superior" strains, $j > i$. Finally, v_i represents the "virulence", or host/patch death rate as a result of infection/occupancy by strain/species i; u is the death rate from all other causes.

Nowak & May (1994) give an extended discussion of eqn (1) for general values of s, combining analytic results with numerical studies of particular s-values. To keep things managable, in this paper we henceforward put $s = 1$. That is, we have a hierarchy of competitively dominant strains/species, such that a strain/species "takes over" a host/patch occupied by an inferior "strain/species" exactly as if that host/patch were uninfected/empty. Furthermore, from now on we will write "species", whether refering to an infecting strain or a metapopulation species.

Putting $s = 1$ in eqn (1), and using $\Sigma_{j=0}^{n}\,y_j = 1$ to write $y_0 = 1 - \Sigma_{j=1}^{n}\,y_j$, we can re-express eqn (1) as

$$\frac{dy_i}{dt} = y_i\left[(b_i - u - v_i) - b_i y_i - \sum_{j=i+1}^{n} y_j(b_i + b_j)\right]. \quad (2)$$

This is our basic equation.

3. Equilibrium Solutions of the Basic Model

Equilibrium solutions of eqn (2) are found by putting $dy_i/dt = 0$, for all i. These equilibrium solutions, y_i^*, are clearly [see also Tilman (1994)]

$$y_i^* = 1 - (u + v_i)/b_i - \sum_{j=i+1}^{n} y_j^*(1 + [b_j/b_i]), \quad (3)$$

if $y_i^* > 0$, and

$$y_i^* = 0, \quad (4)$$

otherwise.

In Nowak & May (1994), we gave a rigorous and general proof (valid for all s, not just $s = 1$) that eqns (3) and (4) give a unique, stable equilibrium solution to the system of equations (2), in the special case where all b_i are equal, $b_i = b =$ constant. More generally, for arbitrary b_i, eqns (3) and (4) can be seen still to represent the unique, stable solution to eqns (2) in the particular case $s = 1$, to which our attention is restricted in the present paper. This result is established by noting that all the sub-diagonal elements of the matrix A defined by equation (11) in Nowak & May (1994) are zero when $s = 1$. In the general case when $s \neq 1$, we have no such proof of stability and uniqueness, and the dynamics can indeed be quite wild (see Nowak & May, 1994 for further discussion).

In eqn (3), notice that there are no solutions for $v_i > b_i - u$. Let $i = n$ represent the first (i.e. largest) v_i with $v_i < b_i - u$. Then

$$y_n^* = 1 - (u + v_n)/b_n. \quad (5)$$

It is now straightforward to compute successive values of y_i^* in terms of the $\{y_j^*\}$ lying above them on the v-axis. It is, however, useful to get a more explicit solution, as follows. Define

$$S_k = \sum_{j=k}^{n} y_j^* \quad (6)$$

and

$$J_k = \sum_{j=k}^{n} y_j^* b_j. \quad (7)$$

Equation (3) can now be rewritten as

$$b_i y_i^* = \sigma_i - b_i S_{i+1} - J_{i+1}. \quad (8)$$

Here, for notational convenience, we have defined

$$\sigma_i = b_i - u - v_i. \quad (9)$$

By analogy with eqn (8), we could also write

$$b_{i-1} y_{i-1}^* = \sigma_{i-1} - b_{i-1} S_i - J_i. \quad (10)$$

Subtracting eqn (10) from eqn (8) we have

$$b_i y_i^* - b_{i-1} y_{i-1}^* = \sigma_i - \sigma_{i-1}$$
$$- b_i S_{i+1} + b_{i-1} S_i + b_i y_i^*. \quad (11)$$

Rearranging this eqn (11), we end up with

$$b_{i-1} S_{i-1} - b_i S_{i+1} = \sigma_{i-1} - \sigma_i. \quad (12)$$

This is an explicit equation, which gives S_i—and thence y_i^*—by trivial iteration.

Before proceeding to focus on the special cases when $b_i =$ constant (case I) and $v_i =$ constant (case II), we make two further simplifications in our notation. First, since all of what follows is focused on equilibrium, we henceforth omit the asterisks: y_i means the equilibrium solution (y_i^* above). Second, and without loss of generality, we put $u = 0$.

3.1. CASE I: EQUAL COLONIZING ABILITY

This limiting case, $b_i = b =$ constant, for all i, was used by Nowak & May (1994). In the superinfection models, it corresponds to all species being equally transmissible; the competitively dominant strains are more virulent (v_i increases as i increases), but all have the same b_i-value. In a metapopulation context, this is a less reasonable limit; it corresponds to all species being equally mobile (so that the inferior competitiors must compensate by, on average, having their patches "live longer").

If all b_i are the same, we can without loss of generality put $b_i = 1$, and eqn (12) reduces to

$$y_i + y_{i-1} = v_i - v_{i-1}. \tag{13}$$

This can be seen to be equivalent to Tilman's (1994) equation (12). Alternatively, we define

$$\Delta v_i = v_i - v_{i-1}, \tag{14}$$

to write

$$y_{i-1} = \Delta v_i - y_i. \tag{15}$$

We see that a newly arising mutant species, with a virulence v_{i-1}, will find it impossible to establish itself if $\Delta v_i < y_i$. That is, invasion and establishment is possible only if the "virulence gap", Δv_i, between the new species and the existing once above it in the "virulence spectrum" or v-axis is big enough, $\Delta v_i > y_i$. This echos Tilman's (1994) theme of "limiting similarity".

Equation (15) is the algebraic form of the illuminating geometrical construction for equilibrium abundances, $\{y_i\}$, illustrated in Fig. 1. This figure again makes it clear that new species cannot establish themselves unless Δv_i is sufficiently large (in relation to y_i).

3.2. CASE II: EQUAL DEATH RATES

This limiting case, $v_i = v_0 = $ constant, for all i, was used by Tilman (1994). In his multispecies metapopu-
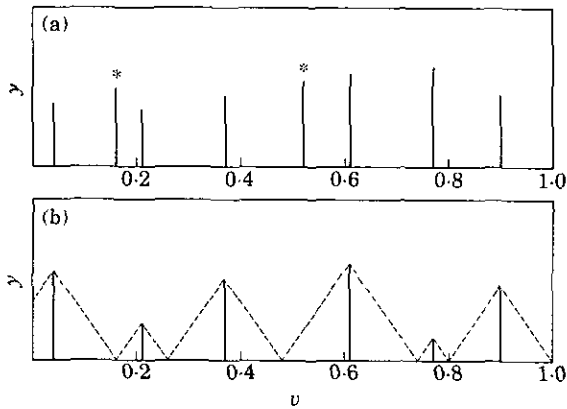

FIG. 1. A simple geometric method is illustrated for constructing the equilibrium configuration, eqns (3) and (4), for the special case 1, when all strains/species have the same dispersal ability [$b_i = $ constant $= 1$; see eqn (15)]. (a) The starting configuration of eight species is shown, located at specific places on the v-axis $(0 < v < 1)$. (b) The equilibrium configuration, is found by constructing a (dashed) line running upwards at 45° to the left from $v = 1$ until it meets the line projected vertically upwards from the location of the strain with the highest v value: $y_n = 1 - v_n$. We then complete the isosceles triangle by projecting a line downwards toward the left from y_n; no species can persist or invade in this "shadow" of y_n [i.e. eqn (15) would give $y_{n-1} < 0$ in this region]. The process is then repeated, as illustrated, to find the abundances of the six species which constitute the equilibrium assembly; two of the initial species [marked with an asterisk in (a)] are eliminated.

lation context, it corresponds to the reasonable assumption that all patches have the same probability of reverting to empty, per unit time, regardless of the species occupying them; that is, the patch death-rate is set by external, environmental effects. The inferior competitors must compensate by being more mobile (b_i decreases as i increases). In a superinfection context, this assumption is unattractive: it implies that all strains affect host lifespan equally, and so the inferior competitors must compensate by being more transmissible.

If all $v_i = v_0 = $ constant, we write eqn (9) for σ_i as $\sigma_i = b_i - v_0$, and the general eqn (12) reduces to

$$\frac{b_{i-1}}{b_i} = \frac{[1 - S_{i+1}]}{[1 - S_{i-1}]}. \tag{16}$$

Notice that the r.h.s. of eqn (15) necessarily exceeds unity, which again underlines the requirement for b_i to increase as i decreases.

Tilman's (1994) work makes various assumptions about the relative abundances of species (i.e. about $\{y_i\}$), and then deduces the consequent expressions for $\{b_i\}$. Equation (16) facilitates such calculations. We, however, are more interested in assuming values for the migration/transmission parameters, $\{b_i\}$, and thence deducing the abundances, $\{y_i\}$, from eqn (16).

For an explicit solution of eqn (16), first define

$$\zeta_k = \frac{b_{k+1}b_{k+3}b_{k+5}\cdots[1, b_n]}{b_k b_{k+2}b_{k+4}\cdots[1, b_n]}. \tag{17}$$

Here, $[1, b_n]$ means whichever of 1 or b_n fits the odd or even sequence in the numerator and denominator of eqn (17). Notice that we have $b_k > b_{k+1}$, for all k, so that $\zeta_k < 1$. With this definition, we can now write the solution of eqn (16):

$$y_i = \zeta_{i+1} - \zeta_i; \quad \text{if} \quad \zeta_{i+1} > \zeta_i,$$

$$y_i = 0; \quad \text{otherwise.} \tag{18}$$

The simplest proof of eqn (18) is by substitution. From eqn (18), $S_k = \Sigma^n_{j=k} y_j = 1 - \zeta_k$. Thus the r.h.s. of eqn (16) is ζ_{i+1}/ζ_{i-1}. But from the definition (17), $\zeta_{i+1}/\zeta_{i-1} = b_{i-1}/b_i$. This is the l.h.s. of eqn (16). QED.

The condition that a newly arising species, with b_i, be able to invade is that $\zeta_{i+1} > \zeta_i$. But, from eqn (17), $\zeta_i = 1/(b_i\zeta_{i+1})$. So the criterion is

$$b_i > (1/\zeta_{i+1})^2. \tag{19}$$

If eqn (19) is not satisfied, $y_i = 0$. This result, eqn (19), can be seen to be equivalent to Tilman's (1994) eqn (10). This criterion does not have any simple intuitive interpretation (in contrast with Fig. 1 for case I).

4. Results About Average Densities and Distributions

So far, we have shown how the equilibrium abundances of the various species, $\{y_i\}$, can be calculated, once the spectra of values of v_i and b_i are specified. In particular, for case I (constant b_i; $b_i = 1$, say), for a given set of v_i-values we can find $\{y_i\}$ from eqn (15). Likewise, for case II (constant v_i; $v_i = v_0$, say), we can find $\{y_i\}$ for a given set of b_i-values from eqn (18). To bring case I and case II into closer formal correspondence, in case II we define the variable $v_i \equiv v_0/b_i$. Then, for both case I and case II, the set of possible strains/species are given by a set of v_i-values, which lie along a continuum of possible values, $0 < v_i < 1$.

Suppose, however, that new species are continually generated by random mutations (or migration, or other mechanisms), with v_i-values in the interval $(0, 1)$. Over time, this will generate some average *distribution* of species, along the v_i-axis; we will be interested both in the average number of species, and in their average abundances, at different places along the v-axis from $v = 0$ to $v = 1$. These distributions will depend both on the probability of a mutant appearing between v and $v + dv$, and on the probability of such a mutant successfully invading.

(i) We define $\rho(v) dv$ to be average number of discrete states, v_i, between v and $v + dv$.

Note that eqn (14) defined $\Delta v_i = v_i - v_{i-1}$. The average value of this quantity, which we call Δv, measures the average spacing between strains/species around $v_i = v$. It follows that

$$\rho(v) = 1/\Delta v. \tag{20}$$

(ii) We define $y(v)$ as the average abundance of any one strain/species in the neighbourhood of $v_i = v$. (It would be interesting to know the distribution of y-values of which $y(v)$ is the mean; for case I, we guess this distribution is Poisson, but we have no proof).

(iii) Finally, we define $x(v) dv$ to be the average total abundance of all the discrete species which have v_i between v and $v + dv$, Clearly,

$$x(v) = \rho(v)y(v). \tag{21}$$

5. Average Total Abundance, $x(v)$

5.1. CASE I: EQUAL COLONIZING ABILITIES OR TRANSMISSIBILITY

Here, eqn (13) gives $y_i + y_{i-1} = \Delta v_i$. On average, this leads to the relation

$$2y(v) = \Delta v. \tag{22}$$

But from eqn (20), $\Delta v = 1/\rho(v)$, whence we have:

$$y(v)\rho(v) = 1/2. \tag{23a}$$

That is, for case I we have

$$x(v) = 1/2. \tag{23b}$$

5.2. CASE II: EQUAL PATCH DEATH RATES OR VIRULENCES

This limiting case requires a little more work. Equation (18) gives us $y_i = \zeta_{i+1} - \zeta_i = \zeta_{i+1} - v_i/\zeta_{i+1}$. But, in this form, it is difficult to see if $v_i < (\zeta_{i+1})^2$, and so on. Therefore we look at

$$y_i + y_{i-1} = \zeta_{i+1} - \zeta_{i-1} = \zeta_{i+1}[1 - v_{i-1}/v_i]. \tag{24}$$

Hence, because $v_{i-1}/v_i < 1$, we know that $y_i + y_{i-1} > 0$.

Using average values in eqn (24), we get the asymptotic expression

$$2y(v) = \zeta(v)[\Delta v/v]. \tag{25}$$

And again using eqn (20) to relate Δv and $\rho(v)$, we arrive at

$$x(v) = \zeta(v)/2v. \tag{26}$$

It remains to calculate the average value of $\zeta(v)$, in the limit of many strains ($n \gg 1$). From the definition of ζ_i, eqn (17), we have

$$\zeta_i = [v_i/v_{i+1}]\zeta_{i+2}. \tag{27}$$

(Remember, we are formally writing $v_i \equiv v_0/b_i$ for case II.) On average, eqn (27) can be re-expressed as

$$\zeta(v - 2\Delta v) = \zeta(v)[1 - (\Delta v/v)]. \tag{28}$$

That is, Taylor-expanding the l.h.s. and cancelling out the Δv factor on both sides,

$$2\frac{d\zeta(v)}{dv} = \frac{\zeta(v)}{v}. \tag{29}$$

Integrating, and noting that $\zeta(1) = 1$, we arrive at

$$\ln[\zeta(v)] = \tfrac{1}{2}\ln(v). \tag{30}$$

That is, $\zeta(v) = v^{1/2}$. Substituting into eqn (26), we arrive at the result for $x(v)$ in case II:

$$x(v) = 1/(2v^{1/2}). \tag{31}$$

5.3. COMPARISON WITH CONTINUOUS LIMITS

It is interesting to compare these results [eqns (23) and (31)] which are obtained directly from the discrete set of equations for the individual $\{y_i\}$ [eqn (2)] with results obtained from a continuous version of eqn (2). Nowak & May (1994) discuss the continuous limit of eqn (2) in the special case when $b_i = $ constant (i.e. case I). More generally, we have from eqn (2):

$$\frac{dy(v)}{dt} = y(v)\left[b(v) - v - \int_v^1 y(s)\rho(s)[b(v) + b(s)]\,ds\right]. \tag{32}$$

Here, as earlier, $u = 0$. An equilibrium solution can be found by putting $dy/dt = 0$, to get

$$b(v) - v = \int_r^1 x(s)[b(v) + b(s)]\,ds. \qquad (33)$$

For *case I*, we put $b(v) = 1$, to get the solution $x(v) = 1/2$. This is the solution obtained this way by Nowak & May (1994), and it is the same as that found directly from analysing the discrete species distribution, eqn (23), above.

For *case II*, we have the formal changes of variables $v \to v_0$ and $b(v) \to v_0/v$, which changes eqn (33) into

$$1 - v = \int_r^1 x(s)[1 + (v/s)]\,ds. \qquad (34)$$

This equation can be seen to have the solution $x(v) = 1/(2v^{1/2})$. This is the result, eqn (31), derived above by more direct methods.

By deriving the continuous results in this way, and comparing them with the appropriate limits from the fully discrete approach (which are known to be the uniquely stable solutions), we have established that these continuous solutions are indeed the (unique) stable ones. There are no stable solutions, in the continuous limit, where finite pieces of the v-axis between v_{min} and v_{max} have $y(v) = 0$ and $x(v) = 0$. This retrospectively ties up some loose ends in Section 6 of Nowak & May (1994).

6. Density of States, $\rho(v)$

This section presents heuristic arguments, on the basis of which we derive a conjectured analytic expression for $\rho(v)\,dv$, the number of species with v_i (or, for case II, $v_0/b_i \equiv v_i$) between v and $v + dv$.

Our underlying assumption is that new mutant strains (for superinfection models, as typified by case I) or new species (for multispecies metapopulation models, as typified by case II) are continuously appearing at some uniform rate, $1/\tau$, such that τ is the average time interval between the appearance of successive new mutant strains/species. We assume that the probability for any one such mutant to appear with v_i between v and $v + dv$ is given by the probability distribution $\pi(v)\,dv$, with v in the interval $(0, 1)$.

We now outline a general, but approximate, argument which derives an expression for $\rho(v)$ in terms of a quasi-equilibrium between "births" and "deaths" of strains/species. Explicit analytic results are derived in the limiting cases I and II, for a variety of specific probability distributions for new mutations as functions of v (namely, $\pi(v)$ uniform, exponentially declining, and harmonic, for $0 < v < 1$). Without loss of

generality, we put $\tau = 1$, so that time can be equivalently measured in terms of the total number of mutants, N, which have appeared up to that point.

These heuristic results for $\rho(v)$ have not been derived in a fully rigorous manner, as will be seen. But, as will be shown in Section 8, they agree very well with extensive numerical simulations. We are encouraged to believe our analytic results are indeed correct, and we hope that some readers will be motivated to provide rigorous proofs of our conjectured results for "death rates", below.

6.1. A "BORN–OPPENHEIMER" QUASI-EQUILIBRIUM APPROXIMATION

As $t \to \infty$, an infinite number of mutations will have appeared ($N \to \infty$), and presumably an infinite number of species will have established themselves.

But at any finite time, we assume the distribution of species will be in rough equilibrium, appropriate to the number of species which are established at time t, $n(t)$. As t increases, we expect $n(t)$ also to increase, but we expect these changes to be slow for very large t, so that for any given total number of species, $n(t)$, the density $\rho_n(v)$ will exist as a quasi-equilibrium (just as electron probability distributions are calculated at quasi-equilibrium, for specified values of the slower-changing configurations of atomic nuclei, in Born–Oppenheimer approximations, and other such "two time scale" approximations).

This quasi-equilibrium is set by the balance between new mutant species appearing and becoming established ("births"), and the consequent reshufflings and removals as newly established species cause the y_i^* of eqn (3) to be rearranged, and some existing species to disappear ("deaths").

6.2. BIRTHS

We have defined the probability for any one new species to appear with v_i between v and $v + dv$ as $\pi(v)\,dv$. But, as the general eqns (3), (4), and the particular expressions for cases I and II [eqn (15) and Fig. 1, and eqns (18) and (19), respectively], make plain, a mutant appearing at $v_i = v$ will not always invade and establish itself; that is, a new mutant will not always have $dy_i(v)/dt > 0$ in eqn (2). So we write $c(v)$ as the probability that, on average, a new mutant appearing at v will be established. Thus the "birth rate", at which new species appear and establish themselves with v_i between v and $v + dv$, is $c(v)\pi(v)\,dv$ (per unit time, measured with $\tau = 1$).

For case I, we see from Fig. 1 that a newly appearing mutant will not persist if it falls within the leftward "shadow" of an existing species, but will succeed otherwise. Thus, on average, $c(v) = 0.5$ for

case I, independent of v. Equivalently, for case I we can see from eqn (15) that the "gaps" into which new mutants can invade scale linearly with Δv (i.e. $v_i - v_{i-1}$) along the v-axis, so that the density of successful invasions is, on average, scaled as [rate of change of v] = constant. For case II in the limit of large $n(t)$, the "gaps" can be seen, from eqns (18) and (30), to scale on average as $\Delta v^{1/2}$ (i.e. $\zeta_i - \zeta_{i-1}$); there is, in a sense, relatively more "gap space" for small v (by virtue of the scaling $v^{1/2}$). For case II, the asymptotic density of successful invasions is thus, on average, scaled as [rate of change of $v^{1/2}$] $= \frac{1}{2}v^{-1/2}$ and $c(v) = \text{constant}/v^{1/2}$.

6.3. DEATHS

Per unit time, the number of species "dying" between v and $v + dv$ depends on: (i) the number of species that are there, $\rho(v)\,dv$; and (ii) the probability that any successfully-established new species will cause the disappearance of a strain at v, $\kappa(v)$. We saw earlier that new introductions affect only species with lower v-values, and not those with higher v-values (because stable states are constructed, as discussed in Section 3 and in Nowak & May 1994, by working "down from the top"). Therefore $\kappa(v)$ will depend on successful establishment of new mutants in the interval $v < v_i < 1$.

We now make a conjecture, which we have *not* succeeded in proving. The conjecture is that the asymptotic probability for any newly-established species to cause a species with $v_i = v$ to disappear, $\kappa(v)$, is proportional to the integrated probability of successful invasion anywhere on the v-interval above v:

$$\kappa(v) = \alpha \int_v^1 \text{"births"}. \tag{35}$$

That is,

$$\kappa(v) = \alpha \int_v^1 c(s)\pi(s)\,ds. \tag{36}$$

Here α is a proportionality constant, $\alpha < 1$, which specifically measures the average probability that a new mutant appearing somewhere in the interval $(v, 1)$ will extinguish a species at v.

For case I and with new mutants equally likely to appear anywhere between $v_{\min}$ and $v_{\max}$ (that is, a uniform probability distribution $\pi(v)$, $\pi(v) = 1$ on $(0, 1)$), we have made direct analytic calculations—based on Fig. 1—of $\kappa(v)$, looking up to the next 15 or so species with $v_i > v$; this suggests eqn (36) is valid, with α around 0·10. More generally, the extensive numerical simulations reported in Section 8 below, suggests that eqn (36) is indeed accurate, particularly

for uniform distributions of new mutations (where we find $\alpha = 0·114$ for both cases I and II in the limit $n \gg 1$).

This being said, eqn (36) remains an unproved conjecture. We hope others will be motivated to work on it. Accepting this conjecture, we have that the average rate at which species are being removed, between v and $v + dv$, is $\rho(v)\kappa(v)\,dv$.

6.4. QUASI-EQUILIBRIUM APPROXIMATION FOR $\rho(v)$

Under the Born–Oppenheimer style of approximation outlined above, we now estimate the quasi-equilibrium value of $\rho(v)$ by setting the rate at which the new mutants successfully establish themselves at v equal to the rate at which existing strains are lost. This birth–death equilibrium is

$$c(v)\pi(v) = \rho(v)\kappa(v). \tag{37}$$

Or, using eqn (36) for $\kappa(v)$,

$$\rho(v) = \frac{c(v)\pi(v)}{\alpha \int_v^1 c(s)\pi(s)\,ds}. \tag{38}$$

Because $c(v)$ appears in both numerator and denominator in eqn (38), it is only the functional dependence of $c(v)$ on v that matters. We put $c(v) = 1$ for case I (constant b_i), and $c(v) = v^{-1/2}$ for case II (constant v_i; thence $v_i \equiv v_0/b_i$), as discussed under Section 6.2 above.

Equation (38) can be written by defining $g(v)$ as

$$g(v) = \int_v^1 c(s)\pi(s)\,ds. \tag{39}$$

Then

$$\rho(v) = -\frac{1}{\alpha}\frac{d(\ln g)}{dv}. \tag{40}$$

The total number of strains/species with $v_i \leqslant v$ may be called $I(v)$. Clearly $I(v) = \int_0^v \rho(s)\,ds$, and so, from eqn (40),

$$I(v) = \frac{1}{\alpha}\ln\left(\frac{g(0)}{g(v)}\right). \tag{41}$$

Here $g(v)$ is defined by eqn (39). The overall total number of strains/species is then $n = I(v_{\max})$; we will return to this in Section 10.

We conclude Section 6 by deriving explicit expressions for $\rho(v)$ for some particular distributions $\pi(v)$, first for case I and then for case II.

6.5. SPECIFIC FORMULAE FOR $\rho(v)$: CASE 1: "SUPERINFECTION"

Here, for a constant transmission rate b_i, we put $c(v) = \text{constant}$ throughout (the value of the constant is immaterial, as it cancels out of our calculations).

6.5.1. Uniform distribution

If new mutations are equally likely to appear anywhere on the v-axis, in the interval $(0, 1)$, then $\pi(v) = 1$. Consequently $g(v) = 1 - v$, and $\rho(v)$ is given simply by

$$\rho(v) = 1/[\alpha(1 - v)]. \tag{42}$$

6.5.2. Exponential distribution

Here we assume that new mutants are more likely to arise with relatively small values of v, as described by an exponential distribution, $\pi(v) = \lambda \, e^{-\lambda v}$. Here $g(v) = \lambda[e^{-\lambda v} - e^{-\lambda}]$, and eqn (38) gives

$$\rho(v) = \lambda/[\alpha(1 - \exp\{-\lambda(1 - v)\})]. \tag{43}$$

In the limit $\lambda \to 0$, we recover the uniform distribution, and eqn (43) reduces to eqn (42).

6.5.3. Harmonic distribution

For reasons which will be discussed under Section 6.6.3 for case II, below, it is also of interest to ask what happens if mutants arise with v_i-values such that $1/v_i$ is uniformly distributed between 1 and some maximum value, $1/\delta \gg 1$. This gives a harmonic distribution for $\pi(v)$ in the interval $(\delta, 1)$, and $c(v)\pi(v) \, dv = a \, dv/v^2$, where a is a normalization constant [which cancels out of eqn (38)]. We get $g(v) = a[(1/v) - 1]$, and

$$\rho(v) = 1/[\alpha v(1 - v)]. \tag{44}$$

6.6. SPECIFIC FORMULAE FOR $\rho(v)$: CASE II: "METAPOPULATIONS"

For case II, as discussed under Section 6.2 above, we put $c(v)$ proportional to $v^{-1/2}$ (again, the proportionality constant cancels out).

6.6.1. Uniform distribution

For $\pi(v) = 1$, we now have $g(v) = 2(1 - v^{1/2})$. From eqn (38), $\rho(v)$ is

$$\rho(v) = 1/[2\alpha v^{1/2}(1 - v^{1/2})]. \tag{45}$$

6.6.2. Exponential distribution

For case II, we have $g(v) = \lambda \int_v^1 s^{-1/2} e^{-\lambda s} \, ds = (\pi\lambda)^{1/2} \, [\mathrm{erf}(\lambda^{1/2}) - \mathrm{erf}(\lambda^{1/2} v^{1/2})]$, with $\mathrm{erf}(z) = 2\pi^{-1/2} \int_0^z \exp(-x^2) \, dx$. It follows that

$$\rho(v) = (1/\alpha)(\lambda/\pi v)^{1/2} e^{-\lambda v}[\mathrm{erf}(\lambda^{1/2}) - \mathrm{erf}(\lambda^{1/2} v^{1/2})]^{-1}. \tag{46}$$

6.6.3. Harmonic distribution

Remember that case II is motivated by the multi-species metapopulation models, and in particular by the special case when all patch death-rates are equal

$(v_i = v_0)$, but with differing dispersal rates, b_i, for different species. To enable us to keep "v" as the basic parameter for this metapopulation "case II", we formally defined $v_i = v_0/b_i$. But this suggests we ought to consider the case when mutant species arise with values of b_i chosen uniformly on some interval (say, v_0 to v_0/δ, with $\delta \ll 1$), which corresponds to a harmonic distribution for v-values on the interval $(\delta, 1)$. As above, we have $\pi(v) \, dv = a \, dv/v^2$, and thence $g(v) = (2/3)a(v^{-3/2} - 1)$. It follows that $\rho(v)$ is given by

$$\rho(v) = (3/2\alpha)[v(1 - v^{3/2})]^{-1}. \tag{47}$$

7. Population Abundance of Individual Strains/Species

In Section 5 we provided exact derivations for the asymptotic total abundances of all species between v and $v + dv$. Specifically, we found $x(v) = 1/2$ [eqn (23)] for case I, and $x(v) = 1/(2v^{1/2})$ for case II [eqn (31)]. And in Section 6 we have given heuristic arguments, leading to explicit expressions for the asymptotic average number of species between v and $v + dv$, $\rho(v) \, dv$; see eqns (42)–(47).

The average population size or abundance of any one species, $y(v)$, is now simply given by eqn (21), repeated for convenience:

$$y(v) = x(v)/\rho(v). \tag{48}$$

Thus, for example, if new mutants arise with v-values that are uniformly distributed along the v-axis, $\pi(v) = 1$, then for case I we have from eqns (23) and (42)

$$y(v) = (\alpha/2)(1 - v). \tag{49}$$

The corresponding expression for case II is, from eqns (31) and (45),

$$y(v) = \alpha(1 - v^{1/2}), \tag{50}$$

and so on.

8. Numerical Simulations

We have also made extensive numerical studies of eqn (2), starting with a few species (with v_i-values drawn from a specified distribution), and letting one randomly chosen mutant appear at each time step (i.e. constant mutation rate, with the average time between mutations being τ, with $\tau = 1$). In effect, we assume the "reshuffling dynamics" are very fast compared to new mutants appearing, because we use the stable equilibrium solutions [eqns (3) and (4)] for

successive ensembles of species, rather than actually following the transient dynamics.

Our procedure is thus as follows. At each time step, a randomly chosen mutant arises (with the v_i-values specified by the probability distribution $\pi(v)$). Equations (3) and (4) tell us whether this new mutant will persist. If it does, existing species may be extinguished, as described by eqns (3) and (4). Time is measured by the total number of mutants that have arisen, $N(t)$: $t = \tau N(t)$. The total number of species present increases slowly, as discussed in Section 10; at any one time, we have an ensemble of $n(t)$ species, characterized by their population sizes $\{y_i\}$ and locations on the v-axis $\{v_i\}$ (for case I, v_i measures virulence or patch death-rate; for case II, v_i is a formal variable, inversely proportional to transmissibility or dispersal rate).

Figures 2 and 3 are for case I, with $\pi(v) = 1$. That is, they correspond to all species/strains having the same transmissibility, and to new mutants having virulence, v_i, equally likely to have any value between v_{min} and v_{max} (normalized to be 0 and 1, respectively); species with higher or lower v_i cannot persist.

Specifically, in Fig. 2 we start with one arbitrarily chosen species, and let the system run until a total of 10^5 mutations have arisen. Starting from the time point when 10^4 mutations have arisen, we sample this system at every 100th time step (after every 100 new mutations). Aggregating all species in bands of v-values of width 0·005 (i.e. in 200 intervals along the v-axis) at each sample point, we compute the average values of $\rho(v)$, $y(v)$ and $x(v)$, as defined above. In Fig. 3 we proceed similarly, but now the system is run for longer, until a total of 10^7 mutations have arisen.

In both Fig. 2 and 3, the dashed lines correspond to the theoretical results: eqn (23) for $x(v)$, eqn (42) for $\rho(v)$, and eqn (49) for $y(v)$. The phenomenological parameter α is estimated from the numerical results for $y(v)$ as a function of v, and this value of α is then used to plot the theoretical curve for $\rho(v)$. Theory and numerical results are in excellent agreement. This is not surprising for $x(v)$, where our theoretical result, $x(v) = 1/2$, is asymptotically exact. But the theoretical curves for $y(v)$ and $\rho(v)$ rest on the heuristic arguments about "death rates" in Section 6.3, and we are surprised that the agreement with numerical results is so good.

We have shown results for both $N = 10^5$ (Fig. 2) and $N = 10^7$ (Fig. 3), to give some idea how the stochastic fluctuations depend on the size of the sample, and thence on how long the system is run.

Figure 4 is for case II, again with the uniform distribution of mutants along the v-axis, $\pi(v) = 1$. In
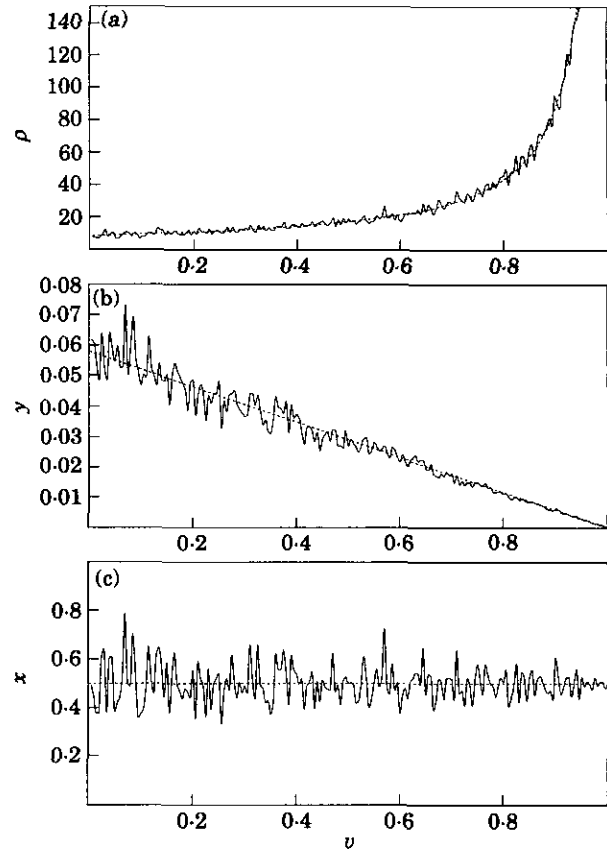

FIG. 2. Theoretical (dashed curves) and numerical (solid curves) results are shown for (a) the average number of strains/species, $\rho(v)$; (b) the average abundance of individual strains/species, $y(v)$; and (c) the total abundance, $x(v)$, respectively, as functions of the variable v which is a measure of virulence, or an inverse measure of dispersal ability). Specifically, these numerical results are obtained by running the system of eqn (2) until a total of 10^5 mutants have appeared ($N = 10^5$), with v-values uniformly distributed along the v-axis and with all strains/species having the same dispersal values (i.e. case I with $\pi(v) = 1$); this corresponds to the "superinfection" metaphor. After 10^4 mutants have appeared, the system is sampled at time intervals corresponding to 100 mutations, and the average values of $\rho(v)$, $y(v)$, and $x(v)$ are computed for each of 200 intervals along the v-axis, spaced 0·005 apart. The theoretical curves come from eqns (42), (49) and (23), respectively. The agreement between the asymptotic theoretical results and the stochastic numerical simulations is good: for $y(v)$, the theoretical parameter α of eqn (36) is set at $\alpha = 0.1159$ by fitting the numerical results; (a) and (c) for ρ and x, respectively, then have no adjustable parameters.

these figures, we have used the intuitive shorthand of calling case I "superinfection", and case II "metapopulation", to reflect the underlying motivation discussed in Section 3. In Fig. 4, the numerical results are obtained exactly along the lines followed for Fig. 3, with again $N = 10^7$. We display $x(v)$, $y(v)$ and $\rho(v)$ as functions of $v^{1/2}$, rather than v, to facilitate comparison with the theoretical results in eqns (31), (50) and (45), respectively.

Although the theoretical expressions for $x(v)$, $y(v)$ and $\rho(v)$ in the "metapopulation" case II are very
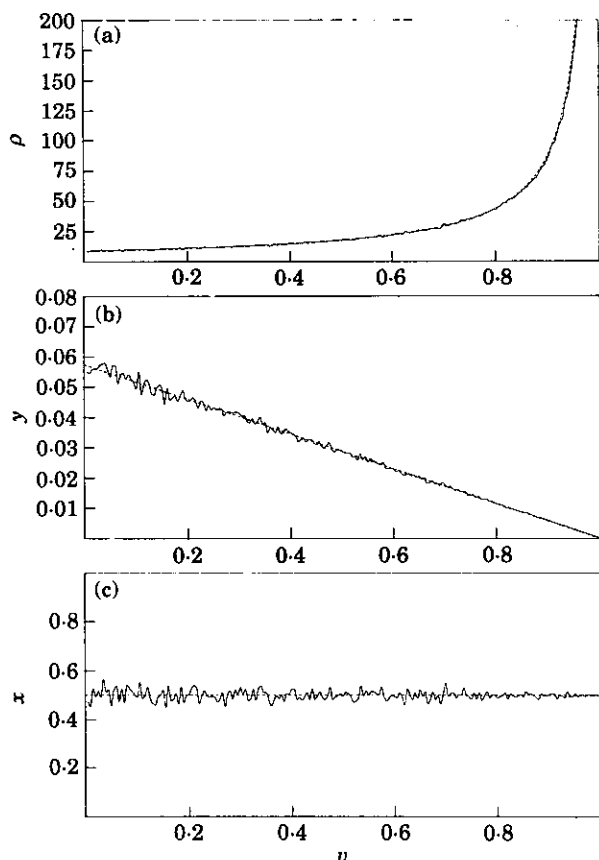
FIG. 3. Exactly as for Fig. 2, except now the system in this superinfection metaphor is run until 10^7 mutants (N) have appeared. Again, the numerical results are obtained by sampling the system at time intervals spaced 100 mutations apart, beginning at the point when 10^4 mutants have appeared, and averaging. The agreement between asymptotic theoretical results and numerical simulations is even better than in Fig. 2, because the stochastic fluctuations are now less noticeable (being reduced by roughly a factor 10, as the number of mutations has increased by a factor 100, compared with Fig. 2). Here $\alpha = 0.1147$.

different from those for the "superinfection" case I, theory and numerical results are again in excellent agreement. As before, this may be expected for our asymptotically exact eqn (31), $x(v) = 1/(2v^{1/2})$, but the agreement with the heuristically based formulae for $y(v)$ and $\rho(v)$ is remarkable. Even more remarkable is the fact that, for the uniform mutant distribution ($\pi(v) = 1$), case I and case II give the same value for the phenomenological parameter α: $\alpha = 0.115$ from Fig. 3 and $\alpha = 0.113$ from Fig. 4.

For the other mutant distributions, such as the exponential and harmonic distributions discussed in Section 6, the agreement between theory and numerical simulations is well within the limits of the numerical fluctuations, and thus looks good, if the system is run up to $N = 10^5$ or so, as in Fig. 2. But, as shown in Figs 5–8, if the system is run long enough for most of the fluctuations to be smoothed out, $N = 10^7$ or

more, the agreement is not as good as it is for the uniform mutant distribution.

Explicitly, Figs 5 and 6 are for the exponential distribution of mutant v-values, for the "superinfection" case I and the "metapopulation" case II, respectively [hence eqns (43) and (46) for $\rho(v)$, respectively]. Figures 7 and 8 are likewise for the harmonic distribution of mutant v-values for cases I and II [eqns (44) and (47) for $\rho(v)$], respectively. In all four cases, the agreement between theoretical and numerical results is not bad—and it is excellent for $x(v)$—but not as good as in Figs 3 and 4. As in Fig. 4, the horizontal axis in Figs 6 and 8 is scaled as
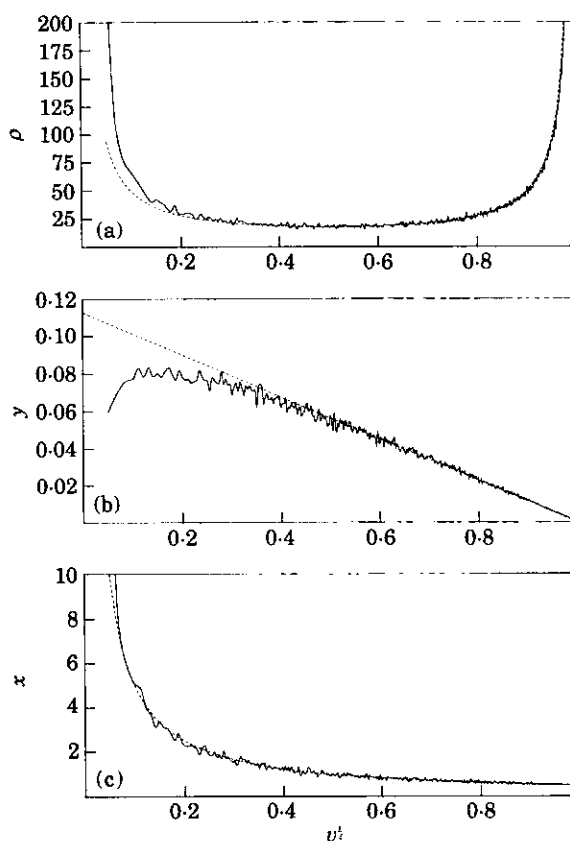

FIG. 4. The numerical results here are obtained exactly as in Fig. 3, by running the system until 10^7 mutations have appeared. The mutation distribution is again uniform along the v-axis ($\pi(v) = 1$), but now we assume the "multispecies metapopulation" metaphor of case II (all species have equal virulence or patch death rates, but different transmissibility or dispersal ability; v is defined formally as $v = v_0/b_i$). The asymptotic theoretical expressions for $\rho(v)$, $y(v)$ and $x(v)$ are here given by eqns (45), (50) and (31), respectively. The one parameter is determined by fitting the theoretical expression for $y(v)$ to the numerical results ($\alpha = 0.1127$), so that the top and bottom figures have no adjustable parameters. Notice that the horizontal axis has been rescaled to be $v^{1/2}$ (not v), as suggested by the theoretical results, eqns (45), (50) and (31). This has the consequence of effectively expanding the v-axis around the origin, so that the stochastic effects seem larger; for very small values of $v^{1/2}$, we have essentially no strains/species. Overall, the agreement between theoretical and numerical results is again excellent, as in the different case illustrated by Fig. 3.
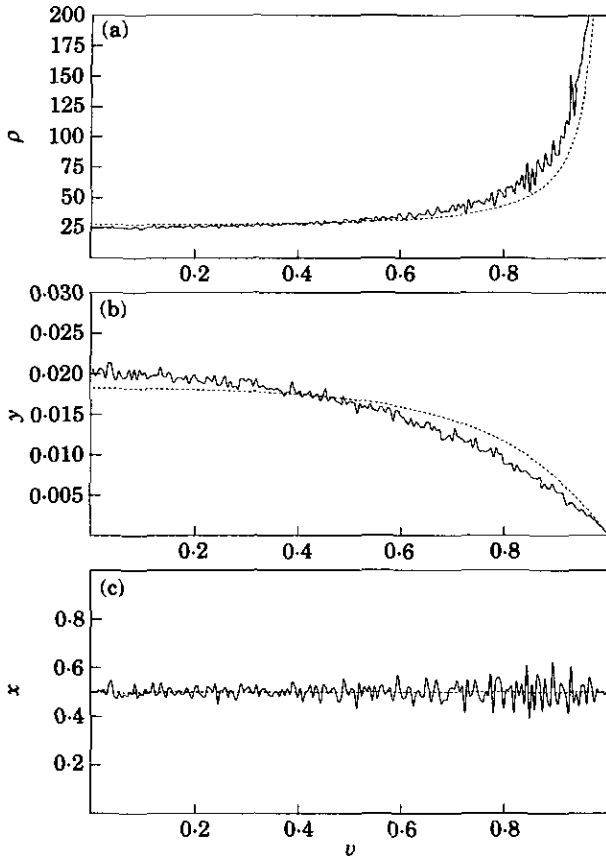
Fig. 5. As for Fig. 3 for "superinfection", case I, but now with the mutation distribution being exponential $(\pi(v) = \lambda\,e^{-\lambda v}$, with $\lambda = 5$ in this example); as in Fig. 3, the system is run until 10^7 mutations have appeared. The asymptotic theoretical results for $\rho(v)$ [eqn (43)], $y(v)$ [from eqn (48)] and $x(v)$ [eqn (23)] are indicated by dashed lines. The phenomenological parameter α is estimated by fitting the theoretical expression for $y(v)$ to the numerical results ($\alpha = 0.1836$; the comparisons for $\rho(v)$ and $x(v)$ thus contain no adjustable parameters. Because fewer mutations appear for larger v-values with an exponential distribution, the results are more noisy as $v \to 1$. As discussed more fully in the text, the agreement between theoretical and numerical results is not bad, but not as good as in Figs 2–4.

$v^{1/2}$, rather than v, to facilitate comparison with the theoretical results; this means the leftwards parts of Figs 6 and 8 are "stretched" relative to Figs 5 and 7, which should be kept in mind when comparing them.

In all cases, the parameter α is estimated from the fit between theory and numerical results for $y(v)$ versus v, so that the theoretical curves for $\rho(v)$ have no free parameters. In summary, these extensive numerical results suggest that our asymptotic analytic results are reasonably reliable, especially when the distribution of mutant v-values is uniform.

9. Relative Abundances of Species

Having established the dynamical properties of these models for superinfection or multispecies meta-

populations, and their evolution over time, we now turn to sketch the implications for species relative abundance (SRA), for total species numbers over time, and for the effects of reducing the number of hosts or patches.

In Tilman's (1994) studies of these systems, an equilibrium distribution of SRA—which was geometric or uniform—was assumed and then the underlying distribution of dispersal/transmission rates, $\{b_i\}$, which would give such an SRA (assuming constant patch death rates, $v_i = v_0$) was deduced.

Here, we deduce the SRA from the basic set of eqns (2), under specified assumptions about the distributions of values of v_i and b_i of the continually appearing mutations. Specifically, for the quasi-equilibrium situation described in Section 6.1, we have information about members of species and about their abundances, as functions of v, contained in $\rho(v)$ and $y(v)$, respectively. From this, we can construct
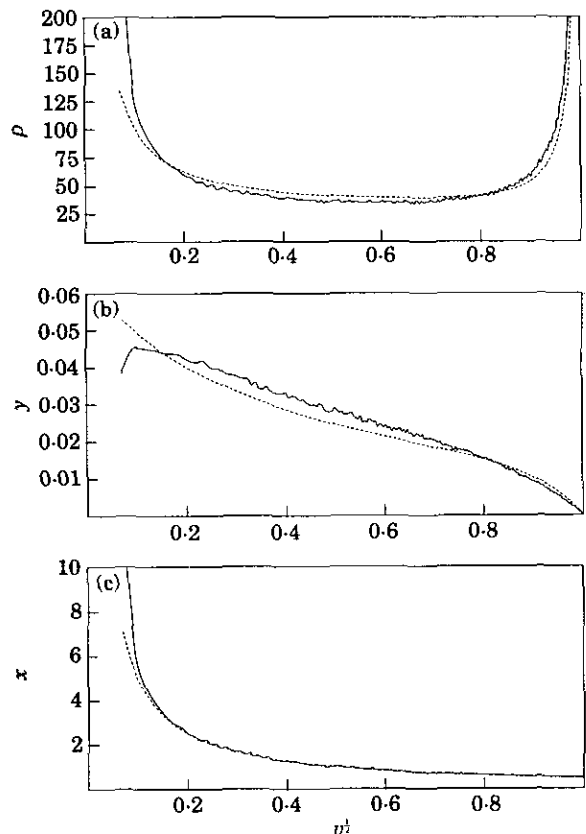

Fig. 6. As for Fig. 5, but now for the "metapopulation" metaphor, case II (again with an exponential distribution of mutations and $\lambda = 5$). The theoretical estimates for $\rho(v)$ [eqn (46)], $y(v)$ [from eqn (48)] and $x(v)$ [eqn (31)] are again represented by dashed lines, and, as in Fig. 4, the horizontal axis is plotted as $v^{1/2}$, as suggested by these theoretical results. The parameter α is estimated from (b) ($\alpha = 0.0791$), and (a) and (c) thus contain no adjustable parameters. The fit between numerical results is excellent for $x(v)$, and reasonable for $\rho(v)$ and $y(v)$.
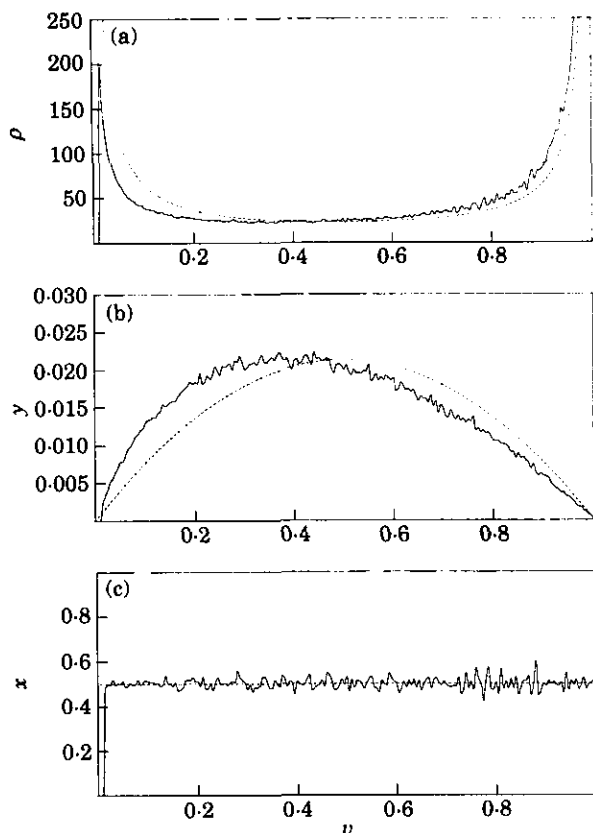
FIG. 7. As for Figs 3 and 5 for the "superinfection" metaphor, case I, run for 10^7 mutations taken from a harmonic distribution ($\pi(v)$ such that $1/v$ is uniformly distributed between 1 and $1/\delta \gg 1$; here $\delta = 0.01$). The dashed lines represent the theoretical results for $\rho(v)$ [eqn (44)], $y(v)$ [from eqn (48)] and $x(v)$ [eqn (23)]. As before α is estimated from (b) ($\alpha = 0.1705$), with no adjustable parameters in (a) and (c). With this harmonic distribution, there is a minimum v-value, $v = \delta = 0.01$, as shown. The agreement between theoretical and numerical results is, as before, excellent for $x(v)$, and not bad for ρ and y.

"rank-abundance" plots, where species are ranked (along the horizontal axis) in descending order of their abundance, while the abundances themselves are plotted on the vertical axes (usually logarithmically). This is a standard way of displaying information about SRA (see, for example, May, 1975).

For our models, things are simpler when $y(v)$ is a monotonic function of v, as it is for both the opposite limiting cases I and II, for most forms of the mutant distributions, $\pi(v)$. Thus, as is seen from Figs 2–8, $y(v)$ decreases monotonically with increasing v for the uniform and exponential distributions (Figs 2–6), although things are more complicated if the distribution of mutant v-values is harmonic (Figs 7 and 8).

In what follows, we mainly restrict attention to the case of a uniform mutant distribution, but considering both of the opposite limits of case I

(constant transmissibility) and case II (constant virulence).

If the abundance of individual species, $y(v)$, indeed decreases as v increases, then the corresponding "rank" is measured simply by the number of species having v-values below v. But this is the quantity $I(v)$ defined by eqn (41). That is, for monotonically decreasing abundance $y(v)$, rank is measured by $I(v)$. For the more general case where $y(v)$ is a unimodal function of v in the interval $0 < v < 1$ (as in Figs 7 and 8), we compute the rank abundance relation as follows: for any given abundance, $y(v)$, less than that of the most abundant species, y_{max}, calculate (from $y(v)$ as a function of v) the two corresponding v-values, v_- and v_+, below and above the value, v_{max}, which gives y_{max}, respectively; the total number of species with abundance greater than $y(v)$—the "rank" of $y(v)$—is then $I = \int_{v_-}^{v_+} \rho(s)\,ds$.
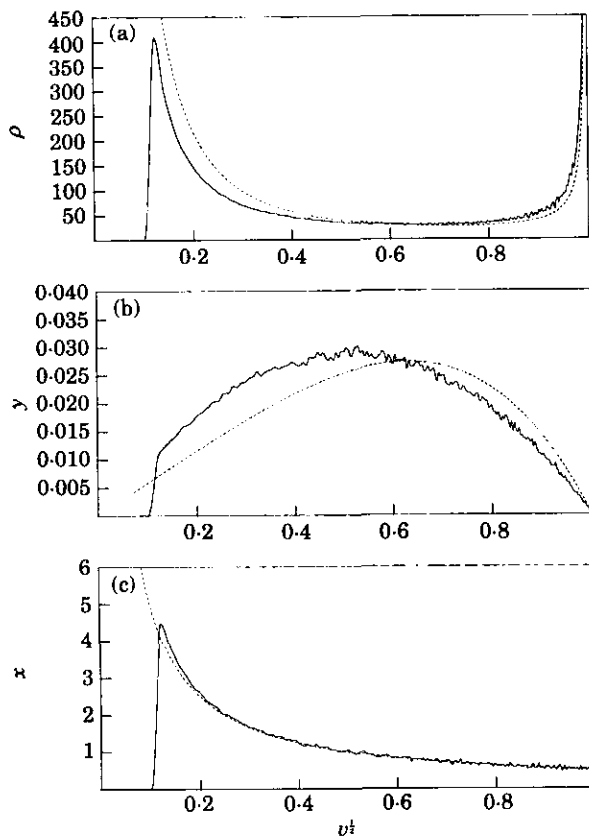

FIG. 8. This sequence of Figs 3–8 is completed by showing the analogue of Figs 4 and 6 for the "metapopulation" metaphor, case II, but now with a total of 10^7 mutations generated by the harmonic distribution defined in Fig. 7. Dashed lines show theoretical estimates for $\rho(v)$ [eqn (47)], $y(v)$ [from eqn (48)] and $x(v)$ [eqn (31)]. For the same reasons as in Figs 4 and 6, the horizontal axis is scaled as $v^{1/2}$, rather than v. Because of this scaling, the minimum value of $v(v = 0.01, v^{1/2} = 0.1)$ is more obtrusive. From (b), we estimate $\alpha = 0.1741$, leaving no adjustable parameters in (a) and (c). As before, theoretical and numerical results are in excellent agreement for $x(v)$, and are reasonable for ρ and y.

CASE I, WITH UNIFORM MUTANT DISTRIBUTION ($\pi(v) = 1$)

In this limit, the $g(v)$ of eqn (39) is $g(v) = 1 - v$, and so the rank-function, $I(v)$, is given by eqn (41) as

$$I(v) = (1/\alpha)\ln[1/(1 - v)]. \tag{51}$$

The corresponding expression for $y(v)$ is given by eqn (49), $y(v) = (\alpha/2)(1 - v)$. We can eliminate the "dummy" variable, v, to get an explicit relation between rank, I, and abundance, y, for this example:

$$I = (1/\alpha)\ln[\alpha/(2y)]. \tag{52}$$

That is, in this basic example, we get a straight line (with negative slope, $-\alpha$) if we plot $\ln$(abundance) against rank.

Figure 9 gives the SRA generated by our numerical simulations of the system of eqns (2), for case I and a uniform mutant distribution. It confirms the analytic result, showing a linear relation between $\ln$(abundance) and rank. Such a relation corresponds to a geometric distribution of SRA.

CASE II, WITH UNIFORM MUTANT DISTRIBUTION
($\pi(v) = 1$)

Here we have $c(v) = v^{1/2}$, so that, from eqn (39), $g(v) = 2(1 - v^{1/2})$, and so, from eqn (41),

$$I(v) = (1/\alpha)\ln[1/(1 - v^{1/2})]. \tag{53}$$

From eqn (50), $y(v) = \alpha(1 - v^{1/2})$. Again eliminating the dummy variable v, we have the rank-abundance relation for this example:

$$I = (1/\alpha)\ln(\alpha/y). \tag{54}$$

This is essentially identical with the corresponding result for case I, as illustrated by Fig. 9.
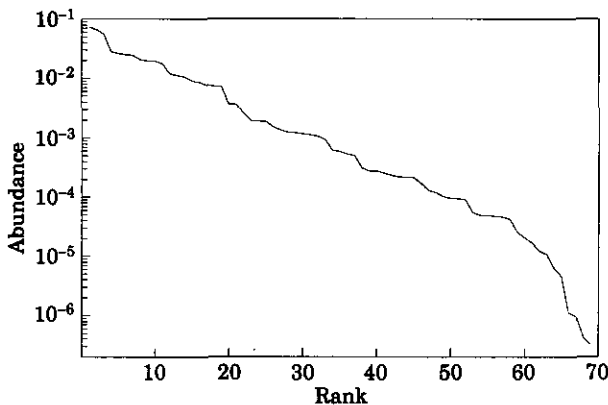

FIG. 9. The rank-abundance relation generated by the "superinfection" metaphor, case I, with mutations arising uniformly along the v-axis. As suggested by the asymptotic theoretical eqn (52), there is a roughly linear relation between the logarithm of abundance (vertical axis) and species rank (i.e. position in the abundance hierarchy, as plotted along the horizontal axis). For a more full discussion, see the text.

Broadly similar patterns are found for exponential distribution of mutants, where the results for $y(v)$ and $\rho(v)$—and thence $I(v)$—are indicated by the theoretical and numerical curves in Figs 5 and 6. For a harmonic distribution of mutants, the theoretical and numerical expressions for $y(v)$ as a function of v are unimodal on (0, 1), rather than monotone decreasing; see Figs 7 and 8. The corresponding rank-abundance relation is calculated along the lines sketched above. For example, for Case I with a harmonic probability distribution of mutants [see eqn (44) and preceding discussion], we have $y = (\alpha/2)v(1 - v)$, and hence $v_+, v_- = (1/2)[1 \pm (1 - y/y_{max})^{1/2}$, with $y_{max} = \alpha/8$. The rank-function, I, is then $I = \int_{v_-}^{v_+} \rho(s)\,ds = (1/\alpha)\ln(v_+^2/v_-^2)$. That is, for this example, the rank abundance relation is

$$I = (2/\alpha)\ln\{[1 + (1 - y/y_{max})^{1/2}]/$$
$$[1 - (1 - y/y_{max})^{1/2}]\}. \tag{55}$$

For y noticably less than y_{max}, eqn (55) reduces to the approximate expression

$$I \approx (2/\alpha)\ln[\alpha/(2y)]. \tag{56}$$

Apart from a handful of the most abundant species, eqn (55) thus also implies a geometric distribution of SRA, similar to eqns (52) and (54) (but with double the slope when $\ln(y)$ is plotted against I, essentially because species abundance falls away on two sides of the peak for a humped $y(v)$ vs. v curve, as in Figs 7 and 8, in contrast to the single side of the peak for the monotone $y(v)$ vs. v curves of Figs 3–6).

We conclude that, in general (and especially if the spectrum of mutations is uniform or close to it along the v-axis), dynamical models of the kind studied here tend, over time, to produce roughly geometric patterns of SRA. Of course, our models emphasize an essentially one-dimensional trade-off, namely, enhanced competitive ability (as reflected by position in the dominance or superinfection hierarchy) versus superior transmissibility and/or lower induced death rate of hosts or patches. A more richly textured set of factors would, other things being equal, tend to compound such geometric distributions, eventually producing a lognormal distribution of SRA once things were sufficiently multifactorial.

10. Total Number of Species as a Function of Time

As our systems of eqn (2) evolve, with new mutant species/strains appearing and sometimes establishing themselves and displacing earlier ones, how many species do we expect to have at time t after the start?

The answer to this question follows immediately from eqn (41) for the asymptotic value of $I(v)$, the number of species with $v_j < v$. The total number of species at time t, $n(t)$, is simply $I(v_{max})$:

$$n(t) = (1/\alpha)\ln[g(0)/g(v_{max})]. \quad (57)$$

Here v_{max} is the v-value of the species closest to the upper limit of unity, and $g(v)$ is defined by eqn (39). For $n(t) \gg 1$, we can write $v_{max} = 1 - \epsilon(t)$, with $\epsilon \ll 1$. Then $g(v_{max}) = \int_{1-\epsilon}^{1} c(s)\pi(s) \, ds \simeq \epsilon c(1)\pi(1)$, and we can write

$$n(t) = (1/\alpha)\ln(a/\epsilon). \quad (58)$$

The constant a is defined as $a = \int_0^1 c(s)\pi(s) \, ds / c(1)\pi(1)$.

It remains to find an explicit expression for $\epsilon(t)$. We first note that, for any single mutation, the probability of being within a small distance ϵ of $v_j = 1$, $p(\epsilon)$, is given by

$$p(\epsilon) = \int_{1-\epsilon}^{1} \pi(s) \, ds. \quad (59)$$

Here we can ignore the complications of establishment, encapsulated in the factor $c(v)$, because—by assumption—such a mutant will be the closest one to $v_j = 1$, and will therefore automatically establish itself. Thus, for $\epsilon \ll 1$, eqn (59) gives

$$p(\epsilon) = \epsilon\pi(1). \quad (60)$$

The corresponding probability that any one mutation will *not* fall between $v = 1 - \epsilon$ and $v = 1$ is $1 - p$. After t trials or mutations, this probability of no mutation falling between $v = 1 - \epsilon$ and $v = 1$ is $(1 - p)^t$, which for $\epsilon \ll 1$ and $t \gg 1$ is e^{-pt}. We may thus define $\epsilon(t)$, the expected difference between v_{max} and 1 after a long time t, as the value of ϵ such that the probability of no mutant having arisen between $1 - \epsilon$ and 1 is 50%: $e^{-pt} = 0.5$. Then, using eqn (60) for $p(\epsilon)$ in the general case of a mutant probability distribution $\pi(v)$, we have

$$\epsilon(t) = (\ln 2)/[t\pi(1)]. \quad (61)$$

Substituting eqn (61) in eqn (58), we have the result

$$n(t) = (1/\alpha)\ln(\gamma t). \quad (62)$$

Here γ is some constant, which depends on the mutant probability distribution, $\pi(v)$, and the asymptotic establishment probability, $c(v)$: $\gamma = \int_0^1 c(s)\pi(s) \, ds / [c(1)\ln 2]$. This result, eqn (62), has been derived under quite general assumptions. It says that the asymptotic total number of species increases as $\ln t$, with time t measured in units of the average interval between mutations, τ (so that we can alternatively

simply count numbers of mutations, $t = N(t)\tau$; usually we put $\tau = 1$).

Figures 10 and 11 give numerical results which confirm the theoretical eqn (62). Figure 10 is for case I ($c(v) = 1$) with a uniform mutation distribution ($\pi(v) = 1$, and so $\gamma = 1/\ln 2$), and it shows—apart from initial transients—a linear relation between total number of species, $n(t)$, and time or, equivalently, number of mutants to have appeared, plotted logarithmically (the figure is based on a very long run, extending to $N = 10^{14}$ mutants).

Figure 11 illustrates some of the underlying features of eqn (62) and Fig. 10, by showing the numbers of species, and their abundances and locations on the v-axis, for snapshots of a representative run (of case I with $\pi(v) = 1$) at $t = 10^3$, 10^4, and 10^5. As is clear from eqn (41) for $I(v)$, the total number of species with v-values up to, say, $v = 0.5$ does not increase with time, once it has reached the long-term average value given by eqn (41). There is reshuffling and fluctuation in the exact locations and abundances of the strains, but $I(0.5)$ remains at around its average value of 6.3. What happens as time, t (and mutations, N), increases is that v_{max} gets closer and closer to $v = 1$, thus adding new species (with low abundances) at the upper end of the v-spectrum; such new additions accumulate slowly, as $\ln t$.

The result of eqn (62), that $n(t)$ scales as $\ln t$, is a robust and interesting one for models of the general kind explored here. We will look at it further in Section 12.
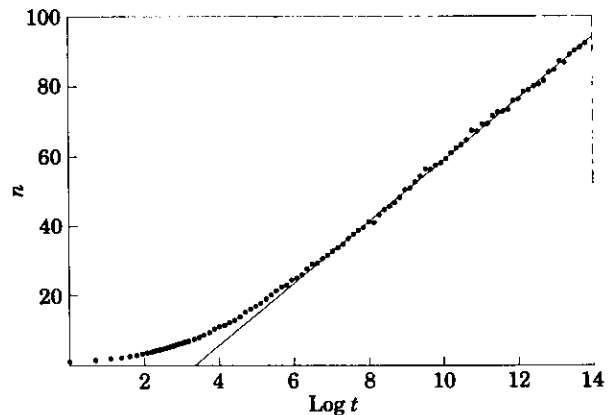

FIG. 10. The number of strains/species arising in the system of eqn (2), $n(t)$, as a function of time, t, or equivalently of the total number of mutations to have appeared ($N = t$, under the normalization that the average time interval between successive mutations, τ, is given by $\tau = 1$). Specifically, this figure is for the "superinfection" case I, with mutations generated uniformly along the v-axis ($\pi(v) = 1$). The extensive numerical simulations follow the system until a total of 10^6 mutants have appeared. The figure shows average values of 100 independent runs. The linear regression is done for the 50 larger values of N. These numerical results are in excellent agreement with the asymptotic expression, $n(t) = (1/\alpha)\ln(t)$, of eqn (60); here $\alpha = 0.114$.
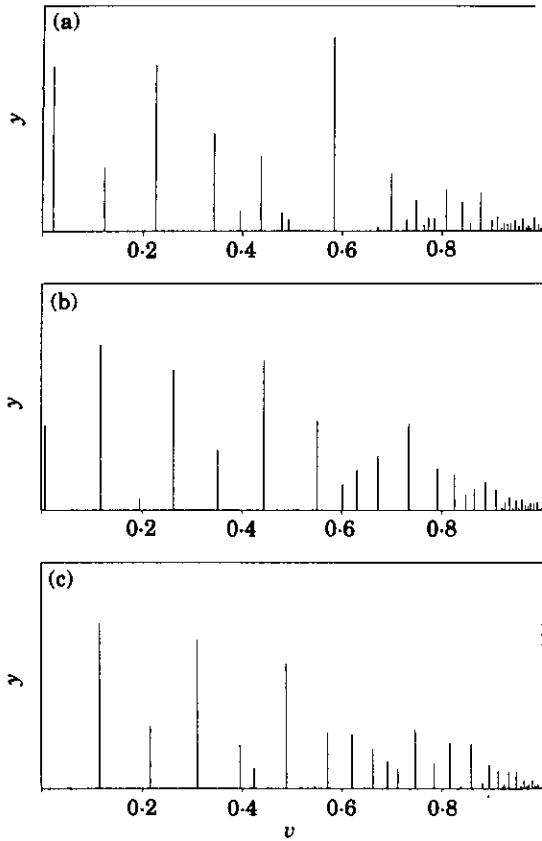
FIG. 11. Here the features underlying Fig. 10 are further amplified. The abundance of the species present, and their location along the v-axis, are shown for the same numerical simulations illustrated in Fig. 10, at the particular times (a) $t = 10^3$; (b) 10^4; and (c) 10^5. The properties illustrated by Fig. 11 are discussed at length in the text.

11. Effects of Reducing the Numbers of Hosts or Habitat Patches

Suppose that in eqn (1) or (2) the total number of hosts, or of available habitat patches, is reduced (by environmental catastrophe, human activities, immigration, or whatever) from the original total of K to some smaller fraction, hK, with $h < 1$. The parameter h thus measures the remaining fraction of hosts or patches. How will such a change affect the total number of strains/species, the average "virulence", and so on?

To answer these questions, we return to our basic eqn (1), and remember that the variables y_i ($i = 0, 1, 2, \ldots, n$) represent the total number of hosts/patches that are susceptible/empty ($i = 0$) or infected/occupied by strain/species i ($i = 1, 2, \ldots, n$), divided by the total number of hosts/patches, K. Thus, in the original state, $\Sigma_{i=0}^{n} y_i = 1$. But if a proportion $1 - h$ are vaccinated/destroyed, then $\Sigma_{i=0}^{n} y_i = h$; under our assumption that transmission/dispersal is homogeneously distributed among all

hosts/patches, the "removed" fraction $1 - h$ of the original hosts/patches are no longer candidates for viable infection or colonization—propagules arriving at these sites "fall on stony ground". For a more extended discussion of this formalism, in the context of vaccination programmes, along with supporting data, see Anderson & May (1991, ch. 5). Nee et al. (1994) discuss how this analysis can be extended, mutatis mutandis, to metapopulation models.

Returning to our basic eqn (2), we now have $y_0 = h - \Sigma_{i=1}^{n} y_i$, and thence

$$\frac{dy_i}{dt} = y_i\left[(hb_i - u - v_i) - b_i y_i - \sum_{j=i+1}^{n} y_j(b_i + b_j)\right]. \quad (63)$$

The stable solutions are thus given by

$$y_i^* = h - (u + v_i)/b_i - \sum_{j=i+1}^{n} y_j^*[1 + (b_j/b_i)], \quad (64)$$

if $y_i^* > 0$, and by

$$y_i^* = 0, \quad (65)$$

otherwise. These equilibrium solutions are exactly as in eqns (3) and (4), except that the first term on the r.h.s. of eqn (64) is now h, not 1.

This implies that the maximum virulence is now reduced, with $[(u + v_i)/b_i]_{max} \leqslant h$. Essentially all our previous results remain valid, with the simple change that "1"—the renormalized limit to the range of v-values in Figs 2–8 and so on (with $u = 0$ and $b = 1$)—is replaced by "h".

Specifically, for case I (the "superinfection" metaphor, with $b_i = $ constant $= 1$) and with a uniform distribution of mutants ($\pi(v) = 1$ on $(0, 1)$), we can again run through the arguments in Section 5, 6 and 7, to get expressions for $x(h, v)$, $\rho(h, v)$ and $y(h, v)$, respectively. Clearly the total abundance of species between v and $v + dv$, $x(h, v) dv$, is exactly as before, for $0 < v < h$:

$$x(h, v) = 1/2. \quad (66)$$

The density of species at $v_i = v$ is now

$$\rho(h, v) = 1/[\alpha(h - v)]. \quad (67)$$

And the average abundance of an individual species at v is

$$y(h, v) = (\alpha/2)(h - v). \quad (68)$$

The species-rank function, $I(v) = \int_0^v \rho(s) ds$, is then given explicitly by

$$I(v) = (1/\alpha)\ln[h/(h - v)]. \quad (69)$$

Combining eqns (68) and (69), the rank-abundance relationship is seen to be

$$I = (1/\alpha)\ln[h\alpha/(2y)]. \tag{70}$$

This differs from the earlier eqn (52) only by the constant factor h in the logarithm. That is, we get a linear relation between rank, I, and $\ln(\text{abundance})$, with the same slope as before, but with the intercept with the vertical axis (the maximum value of $\ln y$) being lower (by the amount $\ln h$).

In general, if the host/patch removal takes place at $t = 0$, then the asymptotic expression for the total number of species, $n(h, t)$, a long time, t, later is again obtained by the arguments given in Section 10 (with "h" consistently replacing "1" as the upper limit to v-values). This gives

$$n(h, t) = (1/\alpha)\ln[y(h)t]. \tag{71}$$

Here, as before, t is measured in units of the average interval between mutations, τ (usually, we put $\tau = 1$, and so $t = N$, the total number of mutations). Equation (71) is identical with the earlier eqn (62), except that the constant $y(h)$ now has the somewhat smaller value $y(h) = \int_0^h c(s)\pi(s)\,ds/[c(h)\ln 2]$. In particular, for case I, with a uniform mutation distribution ($c(v) = 1$ and $\pi(v) = 1$), $y(h) = h/(\ln 2)$.

Thus the most interesting properties of $n(t)$ are asymptotically affected only slightly by removal of hosts or patches: the total number of strains or species, after a sufficiently long time has elapsed, depend logarithmically on t (or, equivalently, on the number of mutations that have appeared). On the other hand, the immediate effect of removing a fraction $(1 - h)$ of all hosts or patches is to cause a marked reduction in the total number of strains/species. Suppose the pristine system has been running for a time t_1, accumulating a total number of species $n(h = 1, t_1)$ given by eqn (62). If a fraction $1 - h$ of all patches are then removed at $t = t_1$, the number of species remaining will be given by integrating the *pristine* expression for the number of states at v, $\rho(h = 1, v)$, from $v = 0$ to the new upper limit at $v = h$:

$$n(h, t_1) = \int_0^h \rho(h = 1, v)\,dv, \tag{72a}$$

$$= (1/\alpha)\int_0^h dv/(1 - v). \tag{72b}$$

That is, immediately after the patches are removed, the remaining total number of species is

$$n(h, t_1) = (1/\alpha)\ln[1/(1 - h)]. \tag{73}$$

Then, as time goes on, the total number of species (with v-values in the interval $(0, h)$) slowly grows—as described by eqn (71) with "t" $= t - t_1$—and new species crowd in close to the upper limit at $v = h$, in the manner indicated by Fig. 11.

Figure 12(a) illustrates these processes. The figure shows the results of numerical simulations for case I with a uniform mutation distribution. ($c(v) = 1$ and $\pi(v) = 1$). After a time $t = 3000$ (i.e. after 3000 mutations have appeared), 50% of all hosts/patches are removed. The result is seen initially to be a marked reduction in the total number of species present, followed by this total then recovering to something close to the previous levels (at equivalent times, or after an equivalent number of mutations). At time
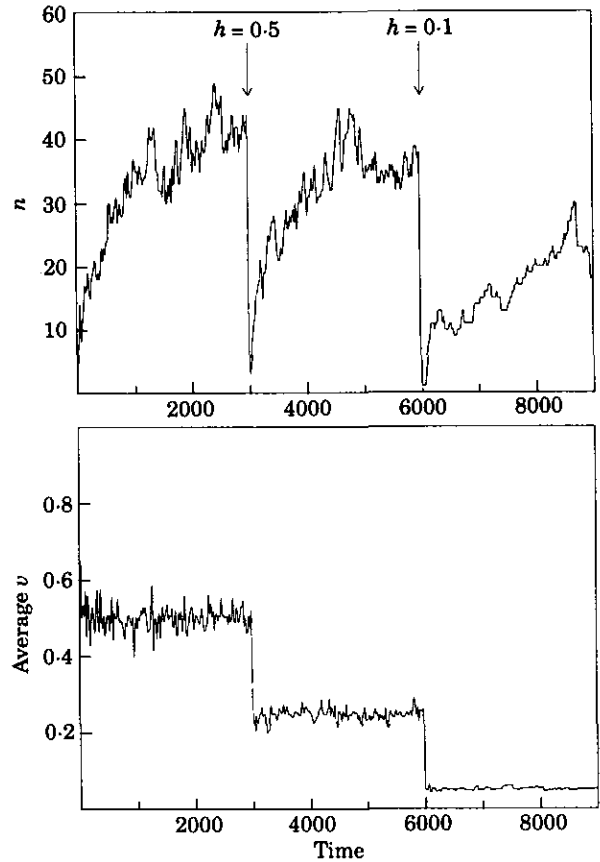

FIG. 12. (a) The number of species present, $n(t)$, as a function of time, t (or, equivalently, number of mutations that have arisen, $N = t$), is shown for the "superinfection" case I, with mutations arising uniformly along the v-axis ($\pi(v) = 1$). At $t = 3000$, the total number of hosts/patches is decreased by 50% ($h = 0.5$); $n(t)$ subsequently increases, until again reduced by removal of 90% of all hosts/patches at $t = 6000$ ($h = 0.1$). Subsequently, $n(t)$ again increases; the somewhat different fluctuation character for $t > 6000$ is because mutations are still arising uniformly along $0 < v < 1$, but only 1/10 of these ($0 < v < 0.1$) now have the possibility of persisting ($V_{max} = 0.1$ for $h = 0.1$). (b) Corresponding average values of the virulence, $\langle V \rangle$, as a function of time, t. Removal of 50% and then 90% of all hosts/patches permanently reduces $\langle V \rangle$ to 0.5 and then 0.1 of its original value. See text for a fuller discussion.

$t = 6000$ (i.e. after a further 3000 mutations have occurred), there is a further reduction in the number of hosts/patches, to 10% of the original total. Once again, there is an immediate marked reduction in the total number of species present, followed by a recovery back toward a higher species total. As described by the theoretical result, eqn (71), this recovery goes as $n(h, t) = (1/\alpha)[\ln(\gamma(1)t) + \ln(h)]$; after equal intervals of time have elapsed, the species totals with $h = 0.5$ and $h = 0.1$ will be lower than the corresponding totals for $h = 1$ by 6 and 20 species respectively (remember, $\alpha = 0.114$ here). Figure 12(a) accords with these theoretical expectations.

Finally, we emphasize that the effects of host/patch removal are significantly to reduce the average levels of virulence. For the "superinfection" metaphor, this means that the effects of vaccination are to remove the most virulent strains, even though vaccination levels may be insufficient to eradicate infection. For the "multispecies metapopulation" metaphor, the corresponding phenomenon is that the inferior competitors, with their compensating greater mobility and/or lower patch death-rates, are favoured by patch removal; this conclusion was previously emphasized by Nee & May (1992) for the two-species case, and extended to multispecies settings by Tilman (1994).

Specifically, the average virulence, $\langle v \rangle$, is given generally by the definition

$$\langle v \rangle = \int_0^{v_{max}} vx(v) \, dv \Big/ \int_0^{v_{max}} x(v) \, dv. \qquad (74)$$

That is, we compute the average value of v, weighted according to the total abundance of species between v and $v + dv$, $x(v) \, dv$. For case I (constant b_i) we have $x(v) = 1/2$, regardless of the mutation distribution, and so

$$\langle v(h) \rangle = h/2. \qquad (75)$$

Thus the effect of removing a fraction $1 - h$ of all hosts/patches is to reduce the average virulence of the remaining strains from $1/2$ to $h/2$. Figure 12(b) illustrates this, applying the results of the numerical simulations shown in Fig. 12(a) to calculate average virulence as a function of time. For case II (constant $v_i = v_0$, and then v defined formally as $v = v_0/b_i$), eqn (74) gives $\langle v(h) \rangle = h/3$, with again a reduction linearly proportional to h.

In summary, removing a fraction of all hosts or patches has relatively little long-term effect on the total numbers of species in these systems, although it does have significant short-term effects. There are, however, persisting implications for the average virulence, or in other contexts, for the average competitive abilities and/or mobility of the species which make up the post-removal community.

12. Conclusions

The bulk of this paper has dealt with analytic and numerical exploration of the dynamical properties of the system of equations (2), as metaphors for superinfection processes among hosts exposed to many different strains of an infectious agent or for the behaviour of multispecies metapopulations. In these models, we have an ensemble of strains or species, with a strict hierarchy of competitive dominance. Inferior competitors possess off-setting advantages in having higher transmission or dispersal rates and/or having lower virulences or patch death-rates. Our emphasis is on the evolution of such systems over time, as new mutants keep appearing. How many species are there? What is their relative abundance? What are the effects of reducing the number of hosts or habitat patches?

Our main conclusions are as follows.

(i) The numerical and analytic results shown in Figs 2–11 suggest that we have built up a good understanding of how the system described by eqn (2) evolves. But the heuristically justified eqn (35), which describes the asymptotic probability that a newly established mutant with $v_i > v$ will cause the disappearance of a species at v, remains a loose end. It is clear from Figs 2, 3 and 4 that eqn (35) is asymptotically accurate when the mutant distribution is uniform ($\pi(v) = 1$), for both the limiting cases I and II, but it would be nice to have a rigorous proof and, if possible, an *a priori* derivation of the phenomenological parameter α ($\alpha = 0.114$ here). For more general mutant distributions, $\pi(v) \neq 1$, Figs 5–8 suggest that eqn (35) is a good first approximation, although a fully accurate treatment is likely to show that α depends (weakly) on v. In short, it would be helpful to have a deeper understanding of the issues summarized in eqn (35).

(ii) As previously emphasized by Tilman (1994), the species whose dynamical interactions are described by equations of the general form of eqn (2) exhibit what an earlier generation of researchers would have called "limits to similarity". A newly arising mutant will not necessarily be able to invade the existing community of species; rather, its values of v_i and b_i need to lie in particular ranges, and not in others, if invasion is to be possible. These allowed ranges depend on the species already present, and are specified by expressions such as eqns (15) and (19) for cases I and II, respectively; Fig. 1 gives a more pictorial version of eqn (15). As time goes on, more

species are slowly accumulated (increasing as ln t), but essentially all of these additions are achieved by increasingly fine division—increasingly close "niche overlap"—among v-values near the upper boundary of the allowed range, Fig. 11 illustrates this point.

Earlier work on "limits to similarity" among competing species tended to deal with questions such as the average separation between species' "utilization functions" along some resource axis, in relation to the intraspecific variance (as reflected in the widths, w_i, of individual such utilization functions; see, for example, May & MacArthur, 1972). But such studies left open the question of what determined w_i, and so—quite apart from other problems—the conclusions did not really provide any basic understanding of how many species we might expect to find packed along such a resource continuum. The models explored in the present paper are different; no limits to similarity are built in. Rather, effective limits emerge, over time, from the evolutionary dynamics of the system. We could start with a stable equilibrium in which an arbitrarily large number of species were evenly (and very closely) spaced along the v-axis, but this initial state would be disrupted by mutations, and would be reshuffled (losing many species in the process) into some configuration more like those illustrated in Fig. 11; even after extremely long times have elapsed (and huge numbers of mutants have come and gone), the species with relatively low v-values (or high b-values; low virulence and/or high transmissibility) will be relatively widely spaced. In these models, moreover, past success is no predictor of persistence, as even the relatively highly abundant and widely spaced species at the low end of the v-spectrum come and go, as a result of reshufflling caused by new mutants invading at high v-values.

Obviously, we recognize that these properties of eqn (2) represent a very abstract metaphor for evolutionary processes. But it seems to be a new kind of such mathematical metaphor, and one with suggestive features.

(iii) One robust conclusion from our models is that, asymptotically, the total number of species increases logarithmically with time [or, equivalently, total number of mutants that have appeared; eqn (62)]. This result holds for both the limiting cases I and II, and is essentially independent of the form of the probability distribution, $\pi(v)$. The result is illustrated in Fig. 10. Disturbance, in the form of a (permanent) reduction in the number of hosts or available habitat patches, causes an immediate marked reduction in the species total, but this total recovers, over time, as illustrated in Fig. 12.

Such an asymptotically logarithmic dependence of the total number of species on time, $n(t) \sim (1/\alpha)\ln t$, could, in practice, be hard to distinguish from $n(t)$ saturating to a constant value. Many trends in fossil records—some of which are read as saturation—could be seen as consistent with species totals tending to rise as ln t.

(iv) Our models evolve toward patterns of species relative abundance that are geometric distributions (i.e. linear relations between rank and ln(abundance)); these results are asymptotically exact if the mutant probability distribution is uniform, $\pi(v) = 1$, and roughly true for more general $\pi(v)$, for both of the opposite limiting cases I and II. As reviewed elsewhere (May, 1975; Begon et al., 1986), such geometric SRA distributions are commonly observed in early succession or in environmentally disturbed situations, arguably because such settings tend to be "ecologically one-dimensional" (in the sense that one set of ecological factors tend to predominate). In our models, there is indeed a one-dimensional character to the trade-offs between competitive dominance and virulence or transmissibility, along our v-axis, but the emergence of a geometric SRA distribution is not trivial or a priori obvious.

(v) Reducing the number of hosts (in the superinfection metaphor) or the number of habitat patches (in the multispecies metapopulation metaphor) favours those species which are lower in the hierarchy of competitive dominance, but which have compensating advantages in greater transmissibility/mobility or in lower virulence/patch death rate. This is intuitively understandable: if there are fewer hosts, then the overall incidence of infection will be lower, and fewer hosts will be multiply infected ("superinfected"); consequently there will usually be less advantage to those strains with intrinsically lower reproductive values, R_0, but which persist because they win in multiply infected hosts.

This observation has implications both for the evolution of virulence in the presence of superinfection, and more generally. First, it suggests that for infections which have many strains with different virulences, and where superinfection occurs, a vaccination programme which has insufficient coverage to eradicate the infection can nevertheless have significant benefits in removing the most virulent strains, and lowering the average virulence [see Fig. 12(b)]. Second, it provides explicit support, in a superinfection context, for the ideas developed by Herre (1993)—and supported by data for nematode parasites of fig wasps—that average virulence is likely to be greater when host density is higher. Third, in the more general context of multispecies

metapopulations, our results suggest that, other things being equal, the species which survive extinction episodes caused by loss of habitat (as in Fig. 12) will be those with better dispersal ability, and not the superior competitors. We are pushing our metaphor much too far in stating that such trends may indeed be seen in some fossil records (e.g. Jablonski, 1994), but we cannot resist it.

REFERENCES

ANDERSON, R. M. & MAY, R. M. (1986). The invasion, persistence and spread of infectious diseases within animal and plant communities. *Proc. R. Soc. Lond.* **B314**, 533–570.

ANDERSON, R. M. & MAY, R. M. (1991). *Infectious Diseases of Humans: Dynamics and Control.* Oxford: Oxford University Press.

BEGON, M., HARPER, J. L. & TOWNSEND, C. R. (1986). *Ecology: Individuals, Population and Communities.* Sunderland, MA: Sinauer.

BREMERMANN, H. J. & PICKERING, J. (1983). A game-theoretical model of parasite virulence. *J. theor. Biol.* **100**, 411–426.

HASTINGS, A. (1986). Disturbance, coexistence, history and the competition for space. *Theor. Popul. Biol.* **18**, 363–373.

HERRE, E. A. (1993). Population structure and the evolution of virulence in nematode parasites of fig wasps. *Science* **259**, 1442–1445.

JABLONSKI, D. (1994). Extinctions in the fossil record. In: *Estimating Extinction Rates* (Lawton, J. H. & May, R. M., eds). Oxford: Oxford University Press, in press.

LEVIN, S. A. & PIMENTEL, D. (1981). Selection for intermediate rates of increase in parasite-host systems. *Am. Nat.* **117**, 308–315.

MAY, R. M. (1975). Patterns of species abundance and diversity. In: *Ecology of Species and Communities* (Cody, M. & Diamond, J. M., eds) pp. 81–120. Cambridge, MA: Harvard University Press.

MAY, R. M. & MACARTHUR, R. H. (1972). Niche overlap as a function of environmental variability. *Proc. natn Acad. Sci. U.S.A.* **69**, 1109–1113.

METZ, J. A. J., DIEKMANN, O. (1986). *The Dynamics of Physiologically Structured Populations. Lecture Notes in Biomathematics,* Vol. 68, Berlin: Springer-Verlag.

NOWAK, M. A. & MAY, R. M. (1994). Superinfection and the evolution of parasite virulence. *Proc. R. Soc. Lond.* **B255**, 81–89.

NEE, S., LAWTON, J. H., LETCHER, A. & HARVEY, P. H. (1994). Animal distributions: patterns and processes. In: *Large Scale Ecology and Conservation Biology* (Edwards, P. J., May, R. M. & Webb, N. R., eds) pp. 41–58. Oxford: Blackwell.

NEE, S. & MAY, R. M. (1992). Patch removal favours inferior competitors. *J. Anim. Ecol.* **61**, 37–40.

TILMAN, D. (1994). Competition and biodiversity in spatially structured habitats. *Ecology,* **75**, 2–16.